Structure−Function Analysis of the Auxilin J-Domain Reveals an Extended Hsc70 Interaction Interface[†,‡]

Jianwen Jiang, Alexander B. Taylor, Kondury Prasad, Yumiko Ishikawa-Brush, P. John Hart, Eileen M. Lafer, and Rui Sousa*

Department of Biochemistry, University of Texas Health Science Center, 7703 Floyd Curl Drive, San Antonio, Texas 78229-3900

Received February 17, 2003; Revised Manuscript Received March 26, 2003

ABSTRACT: J-domains are widespread protein interaction modules involved in recruiting and stimulating the activity of Hsp70 family chaperones. We have determined the crystal structure of the J-domain of auxilin, a protein which is involved in uncoating clathrin-coated vesicles. Comparison to the known structures of J-domains from four other proteins reveals that the auxilin J-domain is the most divergent of all J-domain structures described to date. In addition to the canonical J-domain features described previously, the auxilin J-domain contains an extra N-terminal helix and a long loop inserted between helices I and II. The latter loop extends the positively charged surface which forms the Hsc70 binding site, and is shown by directed mutagenesis and surface plasmon resonance to contain side chains important for binding to Hsc70.

The J-domain is a widespread protein interaction module, conserved from bacteria to humans, and involved in recruiting Hsp70 family chaperone proteins to their sites of action (*1*, *2*). J-domain proteins include *Escherichia coli* Hsp40 and its prokaryotic and eukaryotic orthologues, as well as proteins which typically contain a J-domain as well as a substrate binding domain but lack the gly-phe-rich domain and cys-rich zinc finger characteristic of the Hsp40 co-chaperones (*2*). The substrate binding domains of J-domain proteins function by binding proteins which are then presented to Hsp70 via interactions between Hsp70 and the J-domain. Different J-domain proteins contain distinct substrate binding domains, and it is these domains which, by targeting Hsp70s to specific proteins or protein complexes, confer much of the specificity for the different roles played by Hsp70s in the cell. These include prevention of protein aggregation, facilitation of folding, protein translocation, disassembly of protein complexes, proteolytic facilitation, and even control of regulatory protein activity (*1*, *2*).

One of the best understood of these reactions is the clathrin coat disassembly reaction mediated by Hsc70 (*3*) and auxilin (*4*−*9*). Auxilin is a 910-residue protein composed of an N-terminal cys-rich tensin-like domain, a central clathrin binding domain, and a C-terminal J-domain. Auxilin binds to clathrin-coated vesicles through its clathrin binding domain and then recruits Hsc70 via its J-domain. In a reaction coupled to ATP hydrolysis, auxilin and Hsc70 disassemble the clathrin coat to form a transport vesicle. The location of the J-domain at the C-terminus of auxilin is unusual in that most J-domain proteins, and all Hsp40 orthologues, have the J-domain at the N-terminus (*2*). The structures of three J-domains (from *E. coli* and human Hsp40, and from polyoma virus T-Ag) have been solved by NMR, and one J-domain protein structure (*E. coli* Hsp20) has been solved by X-ray crystallography (*10*−*13*). Despite limited sequence similarity, all four of these structures exhibit canonical 75−79-residue J-domain structures comprising a similar arrangement of four α helices, with helices II and III forming an antiparallel hairpin which contains the invariant HPD J-domain signature motif in the loop between these helices.

Here we describe the crystal structure of an auxilin C-terminal fragment which corresponds to this protein's J-domain. We find that, relative to the canonical J-domain structure, the auxilin J-domain is distinct: it contains an additional N-terminal helix and a long loop inserted between helices I and II. Directed mutagenesis and surface plasmon resonance experiments show that this loop forms part of the functional interface for interaction with Hsc70.

MATERIALS AND METHODS

Expression and Purification of Selenomethionine-Labeled J-Domain. Competent *E. coli* strain B834(DE3) was transformed with a plasmid which expresses bovine auxilin residues 810−910 as part of a GST fusion protein (*5*). Transformed cells were grown in 12 L of M9 media supplemented with selenomethionine to an OD of 0.4−0.7 at 37 °C, and expression of the fusion protein was induced by addition of IPTG to 1 mM. Cells were grown for an additional 3−6 h, harvested by centrifugation, and resuspended in 150 mL of 50 mM Tris pH 8.0, 1 mM DTT, 1 mM EDTA, 1 mM PMSF, and 5% glycerol. Cells were lysed by sonication and 0.05 vol of 10% Polymin P, pH 8.0, was added to precipitate nucleic acid. The lysate was cleared by centrifugation at 15 000 rpm for 15 min, and the supernatant was loaded onto 100 mL of glutathione resin (Pharmacia). The resin was

† Supported by NIH grants NS29051 (to E.M.L.) and GM52522 (to R.S.), Welch Grant AQ-1399 (to P.J.H.), and NIH shared instrumentation grant 1S10RR15883.

‡ Coordinates deposited in PDB 1NZ6.

* To whom correspondence should be addressed. Phone: (210) 567-8782. Fax: (210) 567-8778. E-mail: sousa@biochem.uthscsa.edu.

10.1021/bi034270g CCC: $25.00
Published on Web 04/19/2003

Table 1: Multiple Anomalous Diffraction Data Collection and Phasing Statistics

	Se(peak)	Se(inflection)	Se(low-energy remote)
resolution	50−2.5	50−2.5	50.2.5
wavelength	0.9788	0.9790	0.9813
completeness (%)	100	100	100
R_{merge}	0.054	0.049	0.051
I/σ	37.5	38.9	39.7
phasing power			
acentric (Iso/Ano)	1.68/7.27	2.94/6.51	−/1.89
centric (Iso/Ano)	1.04/−	1.86/−	−/−
R_{cullis}			
acentric (Iso/Ano)	0.69/0.44	0.56/0.38	−/0.94
centric (Iso/Ano)	0.75/−	0.62/-	−/−
overall FOM (acentric)	0.68		
overall FOM (centric)	0.40		

Table 2: Model Refinement Statistics

resolution range	500−2.5
unique reflections	12 866
completeness (%)	98.5 (95.2)[a]
R factor (%)	23.4 (33.4)[a]
R_{free} (%)	26.8 (36.1)[a]
RMSD bonds (Å)	0.007
RMSD angles (°)	1.09
RMSD dihedrals (°)	20.1
RMSD improper (°)	0.827
non-Gly Ramachandran allowed (%)	100

[a] Values for highest resolution shell (2.59−2.50 Å).

washed with 600 mL of 50 mM Tris, pH 8.0, 1 mM DTT, 0.5 M NaCl, 1 mM EDTA, 1 mM PMSF, 0.1% Tween-20, and 5% glycerol, followed by 200 mL of 150 mM NaCl, 50 mM Tris, pH 8.3 ("thrombin cleavage buffer"). A solution of 0.01 mg/mL thrombin in 100 mL of thrombin cleavage buffer was then poured onto the resin, and the resin was incubated overnight at room temperature to allow proteolysis to occur. The cleaved J-domain was then eluted with 100 mL of thrombin cleavage buffer, concentrated to ∼30 mg/mL, and dialyzed into 10 mM Tris, pH 8.0, 1 mM EDTA, 1 mM DTT, and 5% glycerol. After dialysis, tris-2-carboxyethyl-3-phosphine was added to a concentration of 3 mM, and the solution was frozen by dripping into liquid nitrogen and stored at −80 °C.

Crystallization and Data Collection. The protein solution was defrosted at 4 °C and mixed with equal volumes of 20, 22.5, or 25% PEG 8000 and 25% glycerol; 20−40-μL aliquots of the PEG−protein solution were set up as sitting drops at 4 °C and layered with 500 μL of paraffin oil. Crystals nucleated overnight at 4 °C grew to ∼0.2 mM on each edge within a week and were stable for data collection for ∼6 weeks. Crystals were transferred to 15% PEG 8000 and 25% glycerol and flash-cooled by immersion in liquid nitrogen. MAD data on frozen crystals (Table 1) were collected at the X8C beamline at the National Synchrotron Light Source.

Structure Determination. The data were processed with HKL2000, and phasing was carried out with autoSHARP (Table 1). Models were manually built into the density using the program O and were refined with the CNS suite of programs (Table 2). Models of J-domains from yeast and nematode auxilin and human GAK were calculated using bovine auxilin J-domain as a template and the SWISS-MODEL server (www.expasy.org), which uses ProModII and Gromos96 to homology-model and energy-minimize unknown structures using known structures as templates. Molecular graphics for all the figures were prepared with Swiss-PDB Viewer 3.7.

Mutagenesis. Point mutants were prepared by PCR-mediated mutagenesis using the Stratagene Quick-Change kit according to the manufacturer's instructions and a plasmid template expressing bovine auxilin residues 547−910 as part of a GST fusion protein (*5*). Mutations were confirmed by sequencing, and mutant proteins were expressed in BL21-(DE3) *E. coli* grown in rich media and purified as described previously (*7*).

Surface Plasmon Resonance Binding Experiments. Surface plasmon resonance experiments were performed on a BIAcore 3000 surface plasmon resonance instrument utilizing CM5 research grade chips (BIAcore, Piscataway, NJ) as previously described (*7*). GST-auxilin (aa547−910) (wild-type, WT) or indicated mutants were each immobilized at 3200 response units, utilizing amine coupling in 10 mM sodium acetate, pH 5.5. Purified Hsc70 was passed over the surfaces at the indicated concentrations for 30 min, both with and without a 15-min preincubation with 1 mM ATP in buffer A (20 mM imidazole, pH 7.0, 25 mM KCl, 10 mM $(NH_4)_2SO_4$, 2 mM $MgAc_2$, 1 mM DTT, 2 mg/mL CM-dextran, and 0.005% P20). This was followed by a 30-min injection of buffer A, during which time the Hsc70 dissociated from the auxilin-coupled surface. The surfaces were regenerated by a 1-min injection of 1 M GuHCl. An activated and blocked surface was utilized as a reference cell, and the signal from this surface was subtracted from all the data shown. Specificity was documented by the lack of response in the absence of ATP under every condition tested.

RESULTS

Crystallization and Structure Determination of a 101-Residue C-Terminal Fragment of Auxilin. Initial experiments to prepare auxilin J-domain for crystallization used a construct expressing auxilin residues 844−910 as a GST fusion protein (*6*). This fragment corresponds closely in size to the previously determined J-domain structures and contains the invariant HPD sequence at a similar position (30 residues from the N-terminus). It was therefore expected to comprise a structurally intact J-domain. However, this protein was poorly expressed and protease sensitive. A construct expressing residues 810−910 (*5*) was found to give higher yields of stable protein. Selenomethionine-substituted 810−910 fragment was prepared by expression in a methionine auxtotroph and purified by GST affinity chromatography using elution by thrombin treatment to release the GST tag. Purified protein at 15−20 mg/mL was crystallized at 4 °C by microbatch under oil in 10 mM Tris, pH 8.0, 3 mM tris-2-carboxyethyl-3-phosphine, 15% glycerol, and 12.5% PEG 8000. Crystals nucleated overnight and grew to 0.2 mM on an edge in 1 week. The crystals (space group $C222_1$ with $a = 94.1$, $b = 103.1$, and $c = 75.7$ Å) were transferred to 10 mM Tris, pH 8.0, 3 mM TCEP, 25% glycerol, and 15% PEG 8000 and then flash-cooled by immersion in liquid nitrogen. A full MAD data set to 2.5-Å resolution was collected from a single crystal at the X8C beamline at the National Synchrotron Light Source (Table 1). The resulting MAD

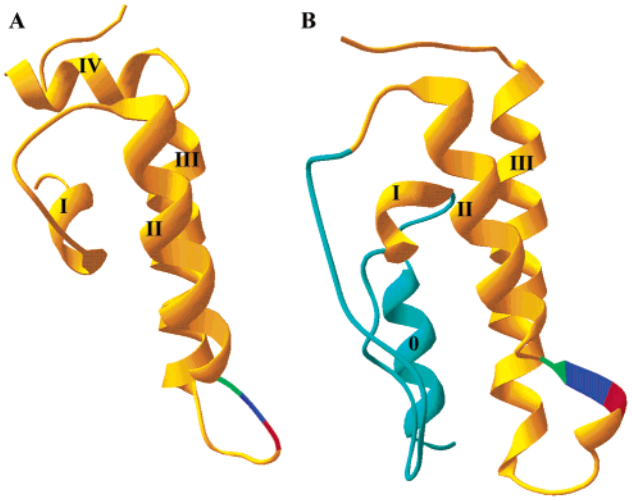

FIGURE 1: Ribbon models of the *E. coli* Hsp40 (A; PDB 1XBL) and auxilin (B) J-domains. Elements common to both J-domain structures (helices I−III) are in yellow, while novel features of the auxilin J-domain (helix 0 and an extra loop between helices I and II) are in cyan. The his, pro, and asp of the HPD J-domain signature motif are in green, blue, and red, respectively.

maps were readily interpretable and revealed two molecules in the asymmetric unit. Only two or three residues at the N-termini of each molecule were disordered, and residues 813−910 and 812−910 were easily built into the density for molecules 1 and 2, respectively. The two molecules are very similar, with an average RMSD of 0.79 Å for all main-chain atoms. The structures, including 21 waters, were refined to an R factor of 23.4% with an R_{free} factor of 26.8% at 2.5-Å resolution (Table 2).

Structure of the Auxilin J-Domain. The auxilin J-domain displays an arrangement of three helices (I, II, and III) similar to that observed previously in other J-domain structures but lacks helix IV (Figure 1). Helices II and III form an antiparallel hairpin linked by the HPD loop and backed by helix I. However, the auxilin J-domain displays an additional N-terminal helix (helix 0) and, most notably, a long loop insertion which connects helices I and II. These "extra" elements form an integral part of the auxilin J-domain: inspection of the structure shows that they contribute a large number of side chains (including three trytophans) to a common hydrophobic core formed together with residues from helices I−III and the HPD loop (Figure 2). This extensive hydrophobic core may contribute to the relatively high T_m (which we found by DSC to be 64.8 °C in 0.1 M sodium phosphate, pH 7.0) of this small, nondisulfide bonded protein domain.

The Extra Loop in the Auxilin J-Domain Is Involved in Binding Hsc70. NMR chemical shift perturbation measurements have mapped the binding site for Hsp70 on *E. coli* Hsp40 to one face of the latter protein's J-domain (Figure 3A; *14*). The residues forming this binding surface are within the HPD loop, helix II, and the short loop connecting helices I and II. This surface is positively charged, and it has therefore been proposed that the J-domain:Hsp70 interaction has a strong ionic component. A surface charge model reveals a similar positively charged site on the corresponding face of the auxilin J-domain (Figure 3B). This positively charged surface is formed, in part, by four lysines (863, 864, 868, 877), an arginine (867), and a histidine (874) from auxilin

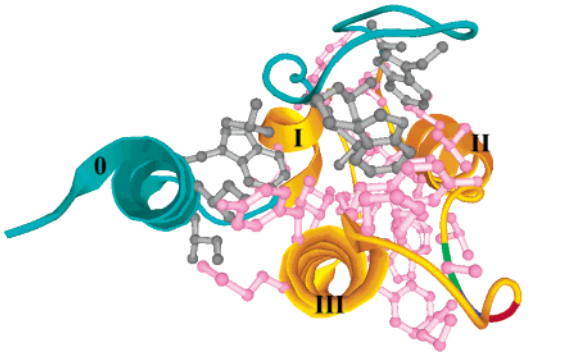

FIGURE 2: Ribbon model of the auxilin J-domain, with side chains forming the hydrophobic core shown in ball-and-stick representation. Coloring of the ribbon follows Figure 1, but the molecule has been rotated 90° so that the HPD loop is closest to the viewer and the C-terminus of helix III is farthest. Side chains from helix 0 and the loop between helices I and II are gray, while those from helices I−III are pink.

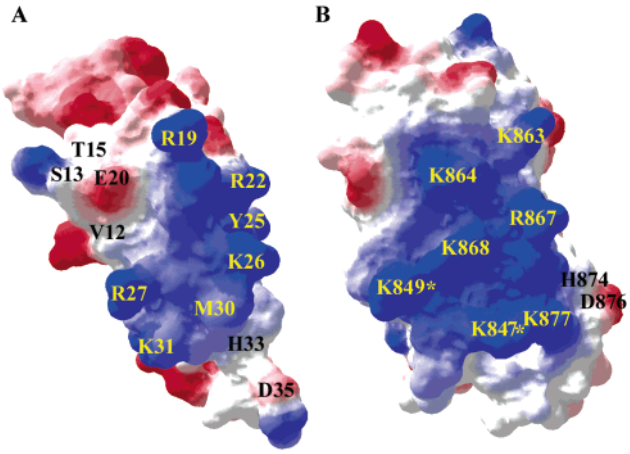

FIGURE 3: Solvent-exposed surface models of the *E. coli* Hsp40 (A) and auxilin (B) J-domains, with positively and negatively charged regions in blue and red, respectively. Orientation of the molecules is as in Figure 1. On the *E. coli* Hsp40 J-domain, the locations of amino acids showing >10-Hz NMR chemical shifts upon binding to Hsp70 are labeled, as are the K847, K849, K863, K864, R867, K868, H874, and D876 residues on the auxilin J-domain structure (residues from the extended loop are indicated with an asterisk).

helix II and the HPD loop. However, lysines 847 and 849 from the long extra loop between helices I and II also contribute to forming this positively charged surface. We therefore hypothesized that K847 and K849 might form part of the Hsc70 binding site.

To test this, we constructed K847C and K849C mutants and evaluated their binding to Hsc70 using surface plasmon resonance. Binding was compared to the WT protein. As a negative control, we also prepared a point mutation (D876A) in the HPD motif. A D35N mutation in the HPD motif of *E. coli* Hsp40 abolishes binding to Hsp70 (*15*), as does a triple alanine substitution of the auxilin J-domain HPD motif (*7*), so we expected that an auxilin D876A mutation would bind Hsc70 poorly or not at all. WT auxilin, K847C, K849C, and D876A were immobilized on separate surfaces of a Biacore chip, and Hsc70 was injected over the surfaces in the presence of ATP. During the time of Hsc70 exposure, we observed a time-dependent increase in the surface plasmon resonance response on all the surfaces except D876A, indicative of Hsc70 binding (Figure 4A). Following termina-

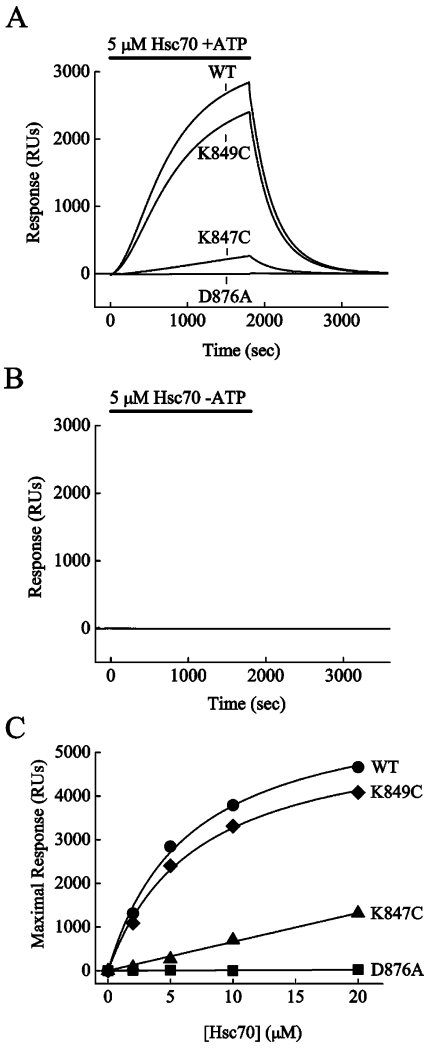

FIGURE 4: Surface plasmon resonance analysis of auxilin mutants. (A) Time course of binding of 5 μM Hsc70 to GST-auxilin (547−910) (WT), K849C, K847C, or D876A in the presence of 1 mM ATP, as monitored by surface plasmon resonance. During the time indicated by the bar, Hsc70 was passed over surfaces to which the indicated auxilin protein had been covalently coupled. (B) Experiment like that shown in (A), except that it was conducted in the absence of ATP. The responses on all four surfaces are superimposed and show undetectable binding. (C) Experiments like that shown in (A) were carried out at different concentrations of Hsc70. The maximal response at the stop of each injection was then plotted as a function of Hsc70 concentration.

tion of the Hsc70 injection, the response returned to baseline as the Hsc70 dissociated from the surfaces. The magnitude of the responses indicated that Hsc70 bound almost as well to the K849C surface as to the WT surface. However, the binding to the K847C surface was dramatically reduced. The binding that was measured was ATP-dependent (Figure 4B) and dose-dependent (Figure 4C). These experiments indicate that K847 forms a critical part of the Hsc70 binding site.

Modeling of Other Auxilin J-Domains. Previous sequence comparisons aligned helix I of the known J-domain structures with auxilin residues 848−852 (*2*, *11*). However, the presence of a long loop between helices I and II of the auxilin J-domain instead aligns helix I of the Hsp40 J-domains with auxilin residues 831−835, as shown in Figure 5. Figure 5 also displays alignments with auxilin homologues from nematode and yeast, and with a nonneuronal human homologue (GAK). Inspection of these alignments does not immediately support the idea that the positively charged residues in helix II and in the loop between helices I and II are critical for binding Hsc70, because only two of the six positively charged residues between 847 and 873 in bovine auxilin are conserved in all four auxilin homologues. However, it is striking that, while individual residues may vary, all four sequences display eight positively charged residues in the segment corresponding to bovine auxilin 847−877. We therefore wondered whether these molecules might all present similar positively charged Hsc70 binding surfaces. To test this, we modeled the structure of the yeast (*8*, *16*), nematode (*9*), and GAK (*17*) J-domains using the auxilin J-domain as a template. Surface charge models of these energy minimized structures are presented in Figure 6 in the same orientation as that used for the bovine auxilin J-domain in Figure 3. As can be seen, all four J-domains display similar positively charged surfaces which present charged side chains at similar positions in space, even when those amino acids may not align in the primary sequence.

DISCUSSION

The structure of the bovine auxilin J-domain reveals that the structural variation among J-domains is greater than we had anticipated. However, despite this structural variation, critical features of the Hsc70 binding site are maintained. In particular, a similar positively charged surface composed of lys and arg side chains lies adjacent to the HPD loop in these J-domain structures. NMR chemical shift perturbation experiments reveal that this electropositive surface forms most of the Hsp70 binding site, at least in *E. coli* Hsp40 (*14*). The binding site for the J-domain in the Hsp70 protein is less well-defined, but mutagenesis studies identify Hsp70 residues R167, N170, and T173 as important for the Hsp70:Hsp40 interaction (*15*). These residues lie at one end of a groove in the Hsp70 ATPase domain and are adjacent to a cluster of negatively charged residues which could interact with the positively charged site on the Hsp40 J-domain (*18*). The idea that the Hsp70:Hsp40 interaction has a large ionic component is reinforced by observations that stimulation of Hsp70 ATPase activity by *E. coli* Hsp40 is highly salt sensitive (*19*). The surface of the bovine Hsc70 ATPase domain (*20*) is not as negatively charged as that of *E. coli* Hsp70, but it also exhibits a negatively charged patch adjacent to residues (R171/N174/T177 in bovine Hsc70) corresponding to those shown to be important for *E. coli* Hsp70:Hsp40 interactions.

Our surface plasmon resonance experiments confirm that a specific lysine (K847) in the auxilin J-domain positive patch is important for the interaction with Hsc70. This residue (highlighted in red in Figure 5), which is part of the extended loop in the auxilin J-domain, shows an interesting pattern of co-variation with an amino acid which lies two residues N-terminal to the HPD loop (V872 in bovine auxilin; highlighted in blue). In the alignments shown in Figure 5, nematode auxilin and human GAK display an arg (R1249 in GAK; R723 in nematode auxilin) at the position corresponding to bovine auxilin K847, while a val or ala occurs at the position corresponding to bovine auxilin V872. In yeast auxilin, an asn (N604) is aligned with bovine auxilin K847, while a lys (K629) aligns with bovine auxilin V872. However, in the 3-D models, the side chain of yeast auxilin

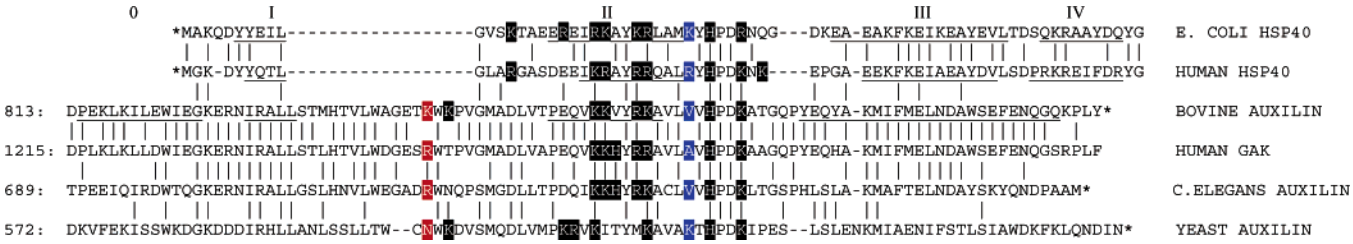

FIGURE 5: Structure-based sequence alignment of human and *E. coli* Hsp40 J-domains with J-domains from bovine, nematode, and yeast auxilin, and a human non-neuronal auxilin homologue (GAK). An asterisk indicates the N- or C-terminus of the protein. Helical regions in Hsp40 and bovine auxilin J-domains are underlined, and positions of helices 0−IV are indicated. Positively charged residues from the putative Hsc70 binding surfaces are highlighted in black, and residues aligning with bovine auxilin K847 and V872 are highlighted in red and blue, respectively.

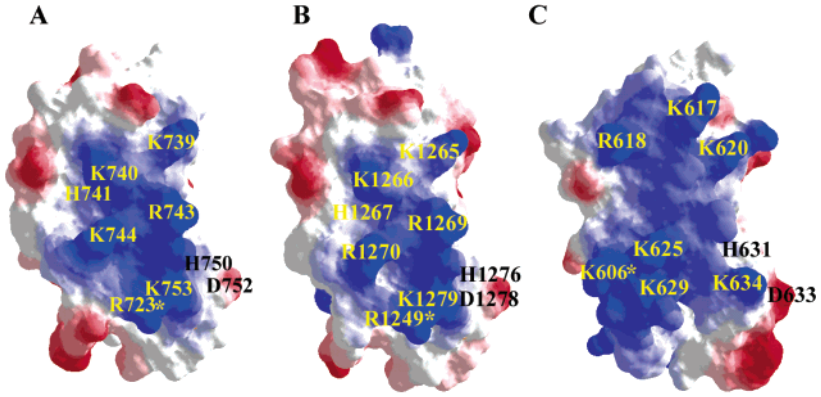

FIGURE 6: Surface charge distribution of nematode (A), human GAK (B), and yeast (C) J-domain structures modeled on the bovine auxilin J-domain structure. Molecular orientation is identical to that in Figure 3. The sequence identity between the bovine auxilin and yeast J-domains is 33%, between bovine auxilin and nematode J-domains it is 56%, and between bovine auxilin and human GAK it is 83%. Labeled residues from the extended loop are indicated with an asterisk.

K629 coincides with those of R1249/R723/K847 in GAK/nematode/bovine auxilin (Figures 3B and 6). In the same way, the side chains of K31/R30 of the *E. coli* and human Hsp40 J-domains coincide with bovine auxilin K847 (Figure 3). Such observations reinforce the functional importance of having a positively charged side chain at this position in the folded J-domain, even when such a side chain is contributed by distinct secondary structure elements which may lie far apart in the primary sequence alignment. However, not all of the residues which contribute to forming this positively charged surface are equally important for binding. Bovine auxilin K849, for example, appears to make minimal contributions to Hsc70 binding. More work is clearly needed to fully define the determinants of the J-domain:Hsc70 interaction.

It is unclear if the distinct structure of the auxilin J-domain contributes to the specific function of auxilin in vesicle uncoating. In some cases it has been shown that J-domains from different proteins are interchangeable. For example, the J-domain of *E. coli* Hsp40 can be functionally substituted with J-domains from the SV40, JC, BK, and polyomaviral T/t antigens, and the viral J-domains can be substituted with J-domains from human Hsp40s (*12*, *21*, *22*). This suggests that structural variation between J-domains may not be functionally critical, though the available structural information also implies that the viral and Hsp40 J-domains are all of the canonical type shown in Figure 1A. In contrast, the J-domain of the cytosolic Sis1p Hsp40 homologue cannot functionally substitute for the J-domain of the Sec63p protein translocase (*23*), so structural variations in J-domains may sometimes modulate interactions with Hsp70-family proteins in a manner important for function. Such effects may be mediated directly, through differences in affinity or the precise mode of binding of the J-domain to the Hsp70 partner, or through differences in how the J-domain is connected to, and communicates with, the substrate binding domain of the protein in which it occurs. Resolution of such questions will depend on further biochemical and structural studies, ideally of J-domain:Hsp70:substrate complexes, as well as on genetic experiments in which structurally distinct J-domains are swapped between different Hsp70 binding proteins.

ACKNOWLEDGMENT

We are grateful to Ernst Ungewickell for supplying us with the wild-type auxilin constructs utilized in this study.

REFERENCES

1. Bukau, B. and Horwich, A. L. (1998) The Hsp70 and Hsp60 Chaperone Machines. *Cell 92*, 351−366.
2. Kelley, W. L. (1998) The J-domain family and the recruitment of chaperone power. *Trends Biochem. Sci. 23*, 222−227.
3. Schlossman, D. M., Schmid, S. L., Braell, W. A., and Rothman, J. E. (1984) An enzyme that removes clathrin coats: purification of an uncoating ATPase. *J. Cell Biol. 99*, 723−733.
4. Ungewickell, E., Ungewickell, H., Holstein, S. E., Lindner, R., Prasad, K., Barouch, W., Martin, B., Greene, L. E., and Eisenberg, E. (1995) Role of auxilin in uncoating clathrin-coated vesicles. *Nature 378*, 632−635.
5. Holstein, E. H., Ungewickell, H., and Ungewickell, E. (1996) Mechanism of Clathrin Basket Dissociation: Separate Functions of Protein Domains of the DnaJ Homologue Auxilin. *J. Cell Biol. 135*, 925−937.
6. Jiang, R.-F., Greener, T., Barouch, W., Greene, L., and Eisenberg, E. (1997) Interaction of Auxilin with the Molecular Chaperone, Hsc70. *J. Biol. Chem. 272*, 6141−6145.

7. Morgan J. R., Prasad K., Jin S., Augustine G. J., and Lafer E. M. (2001) Uncoating of clathrin-coated vesicles in presynaptic terminals: roles for Hsc70 and auxilin. *Neuron 32*, 289−300.
8. Pishvaee, B., Costaguta, G., Yeung, B. G., Ryazantsev, S., Greener, T., Greene, L. E., Eisenberg, E., McCaffery, J. M., and Payne, G. S. (2000) A yeast DNA J protein required for uncoating of clathrin-coated vesicles *in vivo*. *Nat. Cell Biol. 2*, 958−963.
9. Greener, T., Grant, B., Zhang, Y., Wu, X., Greene, L. E., Hirsh, D., and Eisenberg, E. (2001) *Caenorhabditis elegans* auxilin: a J-domain protein essential for clathrin-mediated endocytosis *in vivo*. *Nat. Cell Biol. 3*, 215−219.
10. Pellecchia, M., Szyperski, T., Wall, D., Georgopolus, C., and Wuthrich, K. (1996) NMR Structure of the J-Domain and the Gly/Phe-Rich Region of the Escherichia coli DNAJ Chaperone. *J. Mol. Biol. 260*, 236−250.
11. Qian, Y. Q., Patel, D., Hartl, F.-U., and McColl, D. J. (1996) Nuclear Magnetic Resonance Structure of the Human Hsp40 (HDJ-1) J-domain. *J. Mol. Biol. 260*, 224−235.
12. Berjanski, M. V., Riley, M. I., Anyong, X., Semenchenko, V., Folk, W. R., and Van Doren, S. R. (2000) NMR Structure of the N-terminal J Domain of Murine Polyomavirus T Antigens. *J. Biol. Chem. 275*, 36094−36103.
13. Cupp-Vickery, J. R., and Vickery, L. E. (2000) Crystal Structure of Hsc20, a J-type Co-chaperone from Escherichia coli. *J. Mol. Biol. 304*, 835−845.
14. Greene, M. K., Maskos, K., and Landry, S. J. (1998) Role of the J-domain in the cooperation of Hsp40 with Hsp70. *Proc. Natl. Acad. Sci. U.S.A. 95*, 6108−6113.
15. Suh, W.-C., Burkholder, W. F., Lu, C. Z, Zhao, X., Gottesman, M. E., and Gross, C. A. (1998) Interaction of the Hsp70 molecular chaperone, DnaK, with its co-chaperone DnaJ. *Proc. Natl. Acad. Sci. U.S.A. 95*, 15223−15228.
16. Gall, W. E., Higginbotham, M. A., Chen, C., Ingram, M. F., Cyr, D. M., and Graham, T. R. (2000) The auxilin-like phosphoprotein Swa2p is required for clathrin function in yeast. *Curr. Biol. 10*, 1349−1358.
17. Kimura, S. H., Tsuruga, H., Yabuta, N., Endo, Y., and Nojima, H. (1997) Structure, expression, and chromosomal localization of human GAK. *Genomics 44*, 179−187.
18. Harrison, C. J., Hayer-Hartl, M., Di Liberto, M., Hartl, F.-U., and Kuriyan, J. (1997) Crystal Structure of the nucleotide exchange factor GrpE bound to the ATPase domain of the molecular chaperone DnaK. *Science 276*, 431−435.
19. Ziegelhoffer, T., Lopezbuesa, P., and Craig, E. A. (1995) The dissociation of ATP from Hsp70 of *saccharomyces cerevisiae* is stimulated by both Ydj1p and peptide substrates. *J. Biol. Chem. 270*, 10412−10419.
20. Flaherty, K. M., Deluca-Flaherty, C., and McKay, D. B. (1990) Three-dimensional structure of the ATPase 70K fragment of a heat-shock cognate protein. *Nature 346*, 623−628.
21. Kelley, W. L., and Georgopolous, C. (1997) The T/t common exon of simian virus 40, JC, and BK polyomavirus T antigens can functionally replace the J-domain of the *Escherichia coli* DnaJ molecular chaperone. *Proc. Natl. Acad. Sci. U.S.A. 94*, 3679−3684.
22. Campbell, K. S., Mullane, K. P., Aksoy, I. A., Stubdal, H., Zalvide, J., Pipas, J. M., Silver, P. A., Roberts, T. M., Schaffhausen, B. S., and DeCaprio, J. A. (1997) DnaJ/Hsp40 chaperone domain of SV40 large T antigen promotes efficient viral DNA replication. *Genes Dev. 11*, 1098−1110.
23. Schlenstedt, G., Harris, S., Risse, B., Lill, R. and Silver, P. A. (1995) A yeast DnaJ homologue, Scj1p, can function in the endoplasmic reticulum with BiP/Kar2p via a conserved domain that specifies interactions with Hsp70. *J. Cell Biol. 129*, 979−988.

BI034270G